Geopolymer Concrete: A Sustainable and Economic Concrete via Experimental Analysis

Manvendra verma (mv075415@gmail.com)
Delhi Technological University https://orcid.org/0000-0002-0840-841X
Nirendra Dev
Delhi Technological University

Original Research

Keywords: Geopolymer Concrete, Flyash, GGBFS, Sustainable construction, Mechanical properties

Posted Date: February 11th, 2021

DOI: https://doi.org/10.21203/rs.3.rs-185150/v1

Abstract

Geopolymer concrete is a sustainable, economical, eco-friendly, and high-strength concrete. The GPC utilizes industrial solid wastes like flyash and slag as binding material and is activated by the alkaline solution containing NaOH and Na_2SiO_3 in the design mix. The experimental investigation analyzes both GPC and OPC concrete's physical and mechanical properties for the same mix design and analyzes the concretes cost and sustainability. After the experimental investigation, the GPC and OPC concrete's compressive strength shows similar trends at the 28 days strength, but the initial three days strength of the GPC strength is much higher than the OPC concrete, but around 28 days, the compressive strength of concrete mix got similar. The splitting tensile strength and flexural strength of the GPC specimens are slightly higher than the OPC concrete mix specimens. The OPC concrete's elastic modulus is slightly higher than the GPC mix design, whereas the Poisson ratio of the OPC concrete is slightly lower than the GPC mix designs. The GPC has less embodied energy compared to the OPC concrete. The cost of the GPC at a bulk level reduced the cost of up to 40% of the OPC concrete.

1. Introduction

GPC becomes a perfect alternative to the world's sustainable construction industry because the concrete demand is the second largest in the world after the water. The development of the country and society increases with the increment of the infrastructure. So, concrete production increases exponentially in the future with the development. In the OPC cement production, around a similar amount of carbon emission in the environment to OPC production quantity [1]. The GPC utilizes the Industrial solid wastes flyash and slag in the GPC. Flyash generates in thermal power plants as a waste product in a vast amount, but the utilization of flyash is limited to up to 50% of the production[2]. GPC shows better physical, chemical, and mechanical properties compared to the OPC cement concrete. The durability properties of the GPC are also higher than OPC concrete. GPC is highly resistant to sulfate attack compared to the OPC concrete[3]–[6]. The geopolymerisation reaction plays a vital role in the development of the strength of the GPC. Some factors affect the geopolymerisation process like curing conditions, alkaline solution content, and binding material content in the design mix.

The pozzolanic materials like flyash, GGBFS, metakaolin, and rice husk ash were used as a binding material in the geopolymer due to the high silica, and alumina content composition and compressive strength increases with the increment of Si/Al ratio[7]. The sodium hydroxide and sodium silicate mix solution was used to activate pozzolanic material to work as binding material for the geopolymerisation reaction. The GPC mix's strength increases with the increment of molarity of NaOH, but it reduces the workability[8]–[13]. Geopolymerisation reaction develops the strength of the concrete affected by the various factors and parameters[14]. The alkaline ratio also affects the mix's strength, and it increases with the Na_2SiO_3/NaOH ratio[15].

The curing condition is an essential parameter to gain strength, and the strength increases with the increment of curing temperature up to 100^0C[16][17]. The replacement of flyash by the GGBFS develops

the GPC mix's strength in the ambient curing conditions[18]. The fineness of the flyash plays a vital role in the development of strength, increases the strength, and decreases the mix's setting time [19][20]. The fineness of flyash directly reduces the porosity by increasing small particles in the mix[21][22]. In the geopolymerisation reaction, curing time directly affects the mix's early strength development, and longer curing time gives better end products after the reaction[23]. The water present in the mix was not used in the geopolymerisation endproducts so, evaporation of water from the mixture made the specimens crack-free [24]. The water content increases in the mix reduce the strength of the mix specimens[25]. The flyash and slag have a high potential for reactivity and bond formation for strength development[26]. The GPC has a very high potential to resist the acidic or sea-water environment and other extreme weather conditions[27], and it shows the future scope of the geopolymer paste as a repair of the concrete structure due to their efficiency and performance[28]. The GPC specimens have high stability against the elevated temperature than the OPC concrete samples[29]. Manufacturing sand or stone dust has a high capability to work as fine aggregate in the concrete without reducing their strength. It is also useful in the formation of high-strength GPC[30]. All the building construction constituent's alternative materials embodied energy is lower than the conventional building materials[31]. Embodied energy is used to calculate the carbon footprints used to produce material in various ways[32]. The GGBFS and flyash contents present in the concrete's mix design reduce the concrete's embodied energy [33].

2. Methods

All the constituents used in forming the GPC and OPC concrete specimens for the experimental analysis are explained separately in the paragraphs. The preliminary test on the material samples to identify the concrete laboratory properties in the civil engineering department, DTU, Delhi. The SEM and EDS test of the samples done in the nanotechnology lab, Jamia Millia Islamia, New Delhi, whereas the XRD test in the central facility laboratory, DTU, Delhi. The OPC 43 grade of cement was purchased from the JK cement to experiment with a controlled mix design[34]. In the preliminary check, the cement's quality, by testing consistency, initial and final setting time, specific gravity, fineness of the particles sizes, and soundness. The cement passes all preliminary tests as per Indian standard codes[35]–[40]. Table **1** describes the cement's properties identified through the testing sample in the concrete laboratory in the civil engineering department, DTU, Delhi. Flyash is an industrial solid waste produced from the thermal power plant by the coal ash fumes electrostatic precipitation. The particle size of the flyash somewhat lower or similar to the OPC particle size and contain high silica and alumina in the composition. Flyash brought from the national thermal power plant, Dadri, Gautam Budh Nagar, Uttar Pradesh.

Flyash used for the test is class-c type flyash in the mix design[41]. The particles of the flyash are spherical and porous, confirmed by the SEM image. Fig. 1 shows the amorphous nature of the flyash sample by the XRD graph, whereas Fig. 3 shows the porous spherical particles of the flyash by the SEM image at the 5-micron resolution. Table 2 shows the composition of the chemical constituents present in the flyash explained by the XRF test, and Fig. 4 shows the EDS graph in which describe element content present in the flyash conducted in the nanotechnology lab Jamia Millia Islamia, New Delhi.

GGBFS is produced from the steel manufacturing plant by quenching the slag from the molten iron-steel material. The waste material present in the iron or steel ores is called slag after separating the wastes from the steels' manufacturing. GGBFS also contains the high silica and alumina content in the composition. GGBFS was brought from the Bhilai steel plant, Bhilai, Chhattisgarh, India, to test and produce the GPC mix specimens. Fig. 1 shows the XRD graph of the GGBFS, which shows the sample's amorphous nature, whereas Table 2 shows the chemical composition present in the GGBFS sample. Fig. 2 describes the SEM image of the GGBFS sample at the resolution of two microns and shows the irregular shape of the particles, whereas Fig. 5 shows the EDS graph in which describes the element present in the samples.

2.1.Alkaline Solution

The alkaline solution plays a vital role in the Geopolymerisation reaction because it activates the reaction's pozzolanic binding materials and finds the end products. The alkaline solution contains the sodium hydroxide and sodium silicate solution, and it is mixed before the 20-24 hours for sampling. Sodium hydroxide was purchased from the Fisher scientific manufactured in the business park, Powai, Mumbai, Maharashtra, India. Fig. 6 shows the sample of sodium hydroxide flakes used in the mix design, whereas Fig. 7 shows the sodium silicate sample purchased from the Central Drug House (P) Ltd.

2.2. Aggregates

Aggregate is used as the concrete's skeleton because it occupies up to 85% of the concrete. Various sizes of the aggregate used in the mix are mostly classified into two categories are fine aggregates and coarse aggregates. In the coarse aggregate, two types of aggregates used are 10mm and 20mm in the design mix, whereas in fine aggregate used the crushed stone dust in the mix of both concrete. As per the Indian standard codes, to test the aggregate used quality in the mix design. In the preliminary test, check the gradation of the aggregates, zone, fineness modulus, specific gravity, water absorption, silt content, bulk density, crushing value, impact value, abrasion value, flakiness index, and elongation index of the aggregates samples[42]–[48]. Fig. 8 shows a picture of the raw material of stone dust used as fine aggregate in the mix design. Fig. 9 describes the grain-size curve on the logarithmic graph and the particle size distribution or gradation of the m-sand by the sieve analysis. The stone-dust properties found out through the test conducted in the concrete lab describes in Table 3.

As the percentage passing 600μ sieve is between 35 and 59, the sand belongs to gradation II. From the gradation curve, we find D_{10}=0.1, D_{30}=0.4, and D_{60}=1.2

$C_u = D_{60} / D_{10} = 1.2/0.1 = 12 > 6$

$C_c = D_{30}^2 / (D_{10} \times D_{60}) = 0.4^2 / (0.1 \times 1.2) = 1.33$

Thus the sand is well-graded.

Locally available materials coarse aggregates used in all mixes of concretes. The all particles size of aggregates present in the sample with their percentage and found the coarse aggregate's fineness modulus. **Fig. 10** shows the coarse aggregate sample pic, whereas Table 4 describes the coarse aggregate properties found through the laboratory tests as per the Indian standards[49]–[53]. The fineness modulus of the coarse aggregate is 7.29, calculated through the sieve analysis of the samples.

2.3.Superplasticiser

Superplasticiser is used to enhance the concrete's performance by reducing the mix design's water content and increasing the fresh mix's workability. SNF-based superplasticizer is used in the mix design of both concrete made by the Fosroc industry named SP Conplast-430 in the market[54]. Table **5** shows the properties of the SNF-based superplasticizer used in the mix.

3. Sampling And Test Setup

Specimens made of the controlled OPC concrete mix usually mix all constituents in the pan mixture for around 2 to 5 minutes and cast in the specimens mold for 24 hours. In the case of GPC, the alkaline solution mix before 20-24 hours mixing of the concrete constituents in the pan mixture and cast in the mold of the specimens with the proper compaction of casted samples. The OPC concrete specimens were cured in the water tank, but the GPC specimens were cured in the oven at 60^0C for 24 hours. The cubical, cylindrical, and beam shape specimens cast of both types of concrete for the testing. Physical and mechanical properties tested for both types of concretes. Table **6** describes the mixed proportion of all constituents used in GPC and OPC concretes' mix design.

3.1.Physical properties

The slump and compaction factor test is used for the identification of the workability of the concrete. Slump is most common for testing the concrete's workability in site or laboratory, but the compaction factor is usually used in the laboratory only. Slump is conical in shape, but the compaction factor setup made of the two conical shape buckets fitted in the vertical alignment with a standard gap and down the buckets' surface is openable. The compaction factor checks the self-compaction ability of the concrete with the gravity force[1]. Self-compacting concrete is made with the use of a PCE-based superplasticizer in the concrete mix design[55].

3.2.Density

The weight of the specimens calculates the density of both mixed specimens before the destructive tests. The cube specimen's weight decides the mixes density at the 28 days after the casting, and the mass

calculates the density to volume ratio of the cube specimens[56].

3.3.Mechanical properties test

Compressive strength of both types of concrete mixes tested by the cube sample test under the CTM machine at the 5.25kN/sec rate of the loading statically applied on the specimens. The 150mm*150mm*150 mm' cube sizes as per the Indian Standard code. The mixed samples were tested at 3, 7, 14, 28 days after the specimens casting [56], [57].

Splitting tensile is used to find the indirect tensile strength of the concrete. The cylindrical shape of size diameter*length is 150mm*300mm as per the Indian Standard codes used to find the splitting tensile of the concrete mix specimens. The 4.5kN/sec rate of loading was applied in the transverse direction of the cylindrical specimens for the test of splitting tensile of the concrete[58]. Splitting tensile is higher than the direct tensile but lower to the concrete's same mix design's flexural strength.

Flexural strength is also called a rupture of the concrete used to find the concrete specimens bending capability. If the maximum aggregate size is less than equal to 20mm, then the beam of standard size 100mm*100mm*500mm is used for the cast specimens to analyze the flexural strength. A two-point load was applied along the specimens' transverse direction for the test on the flexural testing machine[59].

Elastic modulus and the Poisson ratio of the concrete mix analyze by testing on the cylindrical specimens. The uniaxial statically load applied along the vertical direction to the cylindrical specimens and found the vertical and horizontal displacement and strength of the cylinder; from the displacements, the Poisson ratio calculated through the ratio of horizontal strain to vertical strain. The elastic modulus finds through the load applied to the cylindrical specimens about one-third of their strength and release and going continuously for the same procedure often draws the stress-strain graph and finds the elastic modulus through the chord modulus as per the American standard code.

3.4 Non-destructive tests

The Non-destructive test is also used to identify specimens' strength without any destruction, and it primarily uses the rebound hammer test and UPV test. Rebound hammer test based on the specimen's surface's penetration reflects by the surface hardness of the specimen[60]. The UPV test propagates the ultrasonic pulse in the sample and measures the time travel duration to pass the specimens. The transducers are connected on two opposite sides of specimens in which one works as an emitter, and another works as a receiver of the ultrasonic pulse wave as per the Indian standard[61].

4. Results And Discussion

All the casted specimens of the mixes of both types of concretes were tested in the machines and compared to concrete mix mechanical properties. The specimens of cubical, cylindrical, and beams were tested as per the Indian standards. The experimental work on the mix of GPC and OPC concrete was

conducted in the concrete laboratory, civil engineering department, Delhi Technological University, Delhi. It includes the slump value, compaction factor, density, compressive strength, splitting tensile, flexural strength Poisson ratio, and elastic modulus done in

4.1.Physical Properties

The slump and compaction factor test is used to analyze the workability of the fresh concrete mix. In both types of concrete, the Slump value of both concrete OPC concrete and GPC are the same 75-100mm, and the compaction factor of the OPC concrete is .89, whereas the GPC is .87 after the mixing in the pan mixture for 3-5 minutes. The concrete mix's workability increases by adding a superplasticizer in the mix without reducing concrete strength [54]. The SNF-based superplasticizer does not harm the GPC specimen's strength [62], [63]. It also increases the microstructure development [64], but it is not beneficial for the elevated temperature[65].

4.2.Density

The concrete sample cubes' weight is used to calculate density before the compressive strength test after the 28 days of casting. The density of the OPC concrete mix design increases with time, whereas the density of the GPC decreases with the same. The maximum density of GPC is 2492kg/m^3 found three days after the casting, whereas the maximum density of the OPC concrete is 2462kg/m^3 found at 28 days after the casting. The concrete density with age is the opposite case in both concrete because the GPC density decreases with increasing time but OPC concrete density increases. Fig. **11** shows the graph between the density and time in which the GPC samples density decreases with increasing time, but OPC concrete density increases with up to 28 days of tests. The density of the concrete increased by the addition of finer content in the mix-like nanoparticles materials.

4.3.Compressive Strength

The compressive strength of the GPC and OPC concretes similar in trends at the 28 days strength, but the initial three days strength the GPC strength is much higher than the OPC concrete but around 28 days the compressive strength of concrete mix got similar. GPC and OPC concrete's three-day compressive strength is 23.2MPa and 14.4MPa, respectively, whereas the 28 days compressive strength of GPC and OPC concrete is 35MPa 35.6MPa, respectively. Fig. **12** shows the graph between the compressive with the time of both concrete. The graph shows the initial strength of the GPC higher than the OPC concrete samples but shows similar strength at 28 days compressive strength. The compressive strength of OPC concrete increases by reducing water content, the addition of superplasticizer, increment of cement content, and silica fumes in the mix design. The compressive strength of the GPC depends on the various parameters are as the molarity of NaOH, alkaline ratio, curing condition, curing temperature, curing time,

water content, and superplasticizer. The compressive strength of the GPC increases with the increment of NaOH concentration in the mix design[66].

4.4.Splitting Tensile Strength

The splitting tensile strength of the concrete mix designs found by the test of the mix design's cylindrical specimens in the compression testing machine at the rate of loading is 4.5kN/sec statically. The splitting tensile strength of the GPC is higher compared to the OPC concrete mix specimens. The splitting tensile of the OPC concrete at 3, 7, 14, and 28 are 1.5MPa, 3MPa, 3.5MPa, and 3.8MPa, respectively, whereas the GPC's splitting tensile at 3, 7, 14, and 28 days are 2.6MPa, 3.2MPa, 3.9MPa, and 4.2MPa respectively. The Splitting strength of the GPC is slightly higher than the OPC concrete for the same compressive strength mix. Fig. **13** shows the splitting tensile of both concrete with the time. It shows that the GPC samples have higher splitting tensile compared to the OPC concrete samples. The GPC specimens show initial high strength at 7 days, but after the 28days show similar trends.

4.5.Flexural Strength

The flexural strength of the concrete mix designs identifies through the testing of the beam samples of the mix design in the flexural testing machine under a two-point load applied on the section of the beam at the transverse direction of the specimens. The flexural strength of the GPC specimens is slightly higher than the OPC concrete mix specimens. The OPC concrete's flexural strength at 3, 7, 14, 28 days is 1.7MPa, 3.4MPa, 3.8MPa, and 4.2MPa, respectively, whereas the GPC flexural strength at 3, 7, 14, and 28 days are 2.8MPa, 3.6MPa, 4.1MPa, and 4.7MPa respectively. Fig. **14** describes the flexural strength with the time of both concrete. It shows the GPC has higher flexural strength to OPC concrete samples at all the time of tests continuously.

4.6.Elastic Modulus and Poisson Ratio

Elastic modulus and the Poisson ratio of the concrete mix design identifies through the test of the cylindrical specimens of the mix in the compression testing machine with vertical and horizontal extension meters. The load was applied along the vertical direction of the specimens statically in the machine. To determine the lateral and linear deformation of the specimens by which got the strains after the failure. The lateral strain ratio to the linear strain shows the Poisson ratio of the concrete mix design, whereas the load applied one-third of failure to the specimens and reduce the load and continue the same procedure many times. The slope of the initial stress-strain curve describes the elastic modulus of the concrete mix designs. The GPC and OPC concrete mix design's elastic modulus was tested 28 days after the casting of the specimens molds. The OPC concrete's elastic modulus is slightly higher than the GPC mix design, whereas the Poisson's ratio of the OPC concrete is slightly lower than the GPC mix designs. The elastic modulus of the OPC concrete and GPC are 26.3GPa and 23.4GPa, respectively, whereas the

Poisson ratio of the OPC concrete and GPC are .15 and .17, respectively. **Fig. 15** shows the elastic modulus of the OPC concrete and GPC at 28 days test of samples. **Fig. 16** shows the setup to determine the Poisson's ratio of the concrete mix cylindrical samples.

Non-Destructive Tests

Rebound Strength

The rebound strength test is generally used in the field as a non-destructive test. It is based on the hammer struck on the specimen's surface with some IS code provisions and showed the rebound value. The Rebound hammer on the specimen surface continuously 10 times, then the rebound gives the average rebound value and gives the rebound strength of the specimens as per the Indian standard. The rebound strength shows similar trends to the mix's compressive strength, but the rebound strength showed a little higher value. The initial three-day strength of GPC higher than the OPC concrete mix but shows somewhat lower strength to the OPC concrete. **Fig. 17** describes the graph of rebound strength of both GPC and OPC concrete.

UPV Test

The UPV test is vital in the non-destructive test method because it directly gives the strength and cracks information in the existing structures. The UPV test needs only two opposite sides of specimens in a clean condition to propagate ultrasonic pulse waves. It plays a vital role in the strength check of the existing damaged or vulnerable structures because rebound tests are based on the surface hardness, so rebound is used only in fewer thickness specimens up to 300mm. The UPV test is mostly used in the consultancy check works of the existing concrete structures. The UPV of the specimens increases with the hardness that directly relates to the strength. **Fig. 18** describes the graph of the UPV test results of both GPC and OPC concrete mix samples. It shows similar trends of GPC and OPC concrete to the rebound strength graph.

TGA (Thermo Gravimetric Analysis)

The TGA test does the thermal analysis of the materials by increasing the temperature 10^0C per second up to 900^0C and check the derivative of weight reduction with the temperature. The apparatus and shows note the weight reduction of the material with increasing temperature in the graphical form. The two-parameter shows in a single graph with different y-axis but in the single x-axis in which one y-axis represents the derivative weight percentage and another one representing the weight percentage reduction with temperature. GPC matrix is highly stable at the elevated temperature without failure compared to the OPC concrete matrix. **Fig. 19** describes the graph of TGA-DTG of GPC concrete up to the temperature of 850^0C. It shows the weight reduction with increasing temperature, but the GPC matrix is highly stable up to 850^0C, and it shows the retained material 92% of the original at 850^0C. DTG graph shows the reduction of the weight with temperature is non-linear, and it varies from negative to positive undefinedly.

Mechanical properties correlation

The correlation generates through the data of mechanical properties produces by the destructive test in the laboratory. The linear regression analysis of data among the compressive strength, splitting tensile, and flexural tensile strength shows the correlation equation and compared it to the Indian standard correlation equations.

Correlation between the compressive strength and splitting tensile

The correlation between splitting tensile and compressive strength proposed eq. (1). It generates through the regression analysis of the data generates by the destructive testing in the laboratory. The ACI committee gives eq. (2) in the state of the art of high strength concrete[67] and a committee of euro code international gives eq. (3) in the model code 1990[68]. eq. (4) introduced by an ACI standard and report for building code requirements for structural concrete[69]. **Fig. 20** describes the graph of the correlation between the compressive strength and splitting tensile. The correlation equation produces by regression analysis of the test data.

$$\text{Proposed: } f_{st} = -.63 + .14 f_{ck} \quad (1)$$

$$ACI363R-92: f_{st} = 0.59\sqrt{f_c} \quad (1)$$

$$CEB-FIP: f_{st} = 0.301 f_c^{0.67} \quad (2)$$

$$ACI\ 318-14: f_{st} = 0.56 f_c^{0.5} \quad (3)$$

Correlation between compressive strength and flexural strength

The correlation between the compressive strength and flexural describes by the eq. (5) generates through the regression analysis of the test data. ACI committee introduces the eq. (6) in the publication of the state of the art of high strength concrete[67]. A standard report presented on the code for the design of concrete in the structure introduces the eq. (7) of correlation[69]. Australian code for the reinforced concrete design presented the correlation eq. (8), and the Indian code introduced the eq. (9) between the flexural strength and compressive strength[70],[71]. The flexural strength is always about 10%-20% of the compressive strength. The tested data also lies between these values. **Fig. 21** describes the correlation equation's graph between flexural strength and compressive strength proposed by the tested data.

$$\text{Proposed: } f_{fs} = -1.03 + .16 f_{cs} \quad (5)$$

$$ACI363R - 92: f_{fs} = 0.94\sqrt{f_c} \quad (6)$$

$$\boldsymbol{ACI\ 318 - 99: f_{fs} = 0.62\sqrt{f_c}} \quad (7)$$

$$\boldsymbol{AS\ 3600: f_{fs} = 0.6\sqrt{f_c}} \quad (8)$$

$$\boldsymbol{IS\ 456 - 2000: f_{fs} = 0.7\sqrt{f_c}} \quad (9)$$

Sustainability Analysis

Sustainable development is essential for the present scenario. A very massive amount of industrial solid wastes produces in the present time requires the usage of that waste in the development work. The usage of industrial solid wastes reduces the carbon footprints, indirectly reduces the usage of the high embodied energy products. The OPC cement's embodied energy produced by the dry process is about 4.6MJ/kg, whereas the flyash and slag have nil embodied energy. The industrial solid wastes flyash and slag used as a binder in the concrete by replacing the OPC and that wastes activated by the chemical solution of sodium hydroxide and sodium silicate. The GPC has less embodied energy compared to the OPC concrete[31]–[33], [72]–[74]. The embodied energy calculation of both concrete is shown in Table **7**. The embodied energy of all constituents of concrete calculated based on reference papers.

Cost Analysis

The concrete cost was calculated by the amount of the constituents present in the concrete mix design, and then, after calculating the rate of all individual constituent prices, the concrete mix design cost was found. The cost of the GPC at a bulk level reduced the cost of up to 40% of the OPC concrete. The cost of the OPC of $1m^3$ is Rs. 3758, whereas the cost of the GPC of $1m^3$ is Rs. 2230. Table **8** describes all calculations of the cost of the materials and concrete. The materials and concrete costs are essential in the construction industries because the construction projects' costs are always higher. The project's economy always matters and goes for the optimum point, which got the essential strength with the project's lesser cost. The GPC is economic concrete compared to the OPC concrete and also reduced pollution or carbon footprints. GPC is a new trend in the construction industry due to sustainable development properties.

Conclusion

After the experimental, sustainability, and cost investigation concluded the followings:-

- In both types of concrete, the slump value of both concrete OPC concrete and GPC are the same 75-100mm, and the compaction factor of the OPC concrete is .89, whereas the GPC is .87 after the mixing in the pan mixture for 3-5 minutes.
- The density of the OPC concrete mix design increases with time, whereas the density of the GPC decreases with the same.
- The compressive strength of the GPC and OPC concretes similar in trends at the 28 days strength, but the initial three days strength the GPC strength is much higher than the OPC concrete but around 28 days the compressive strength of concrete mix got similar.
- The splitting tensile and flexural strength of the GPC is slightly higher than the OPC concrete mix specimens. Similarly, the OPC concrete's elastic modulus is slightly higher than the GPC mix design, whereas the Poisson ratio of the OPC concrete is slightly lower than the GPC mix designs.
- The GPC has less embodied energy compared to the OPC concrete.
- The cost of the GPC at a bulk level reduced the cost of up to 40% of the OPC concrete. The cost of the OPC of $1m^3$ is Rs. 3758, whereas the cost of the GPC of $1m^3$ is Rs. 2230.

Declarations

Funding Statement

This study is supported by the Delhi Technological University, Delhi, India.

Conflict of Interest

There are no conflicts of interest or competing interests in this article.

Author Contribution

All authors have participated in (a) conception and design, or analysis and interpretation of the data; (b) drafting the article or revising it critically for valuable intellectual content; and (c) approval of the final version.

Availability of data and material

The available data had been used and discussed in the manuscript.

Compliance with ethical standard

This manuscript has not been submitted to, under review at, another journal or other publishing venue.

Consent to Participate

As a corresponding author or on behalf of all authors of the research paper, I consent to participate.

Consent to publication

All author of the research paper is consent to the publication.

Acknowledgment

The experimental test was conducted in the concrete laboratory in the civil engineering department of Delhi technological University, Delhi, India. It includes a compressive strength test, splitting tensile, flexural strength, density, slump, Poisson's ratio, and modulus of concrete mix elasticity; the XRD analysis and TGA test conducted in the central facility laboratory of DTU.

References

[1] M. Verma and N. Dev, “Geopolymer concrete : A way of sustainable construction,” *Int. J. Recent Res. Asp.*, vol. 5, no. 1, pp. 201–205, 2018.

[2] Central Electricity Authority, “Flyash generation at coal/lignite based thermal power stations and its utilization in the country,” 2019.

[3] I. Ismail, S. A. Bernal, J. L. Provis, S. Hamdan, and J. S. J. Van Deventer, “Microstructural changes in alkali-activated fly ash/slag geopolymers with sulfate exposure,” *Mater. Struct. Constr.*, pp. 361–373, 2013.

[4] C. Chotetanorm, P. Chindaprasirt, V. Sata, S. Rukzon, and A. Sathonsaowaphak, “High-Calcium Bottom Ash Geopolymer : Sorptivity, Pore Size, and Resistance to Sodium Sulfate Attack,” vol. 25, no. January, pp. 105–111, 2013.

[5] W. Gustavo *et al.*, “Fly Ash Slag Geopolymer Concrete : Resistance to Sodium and Magnesium Sulfate Attack,” *J. Mater. Civ. Eng.*, vol. 28, no. 12, pp. 1–9, 2016.

[6] M. A. R. Bhutta *et al.*, “Sulphate Resistance of Geopolymer Concrete Prepared from Blended Waste Fuel Ash,” *J. Mater. Civ. Eng.*, vol. 26, no. 11, pp. 1–6, 2014.

[7] P. Duxson *et al.*, “Understanding the relationship between geopolymer composition, microstructure and mechanical properties,” *Colloids Surfaces A Physicochem. Eng. Asp.*, vol. 269, pp. 47–58, 2005.

[8] G. Nagalia, Y. Park, A. Abolmaali, and P. Aswath, “Compressive Strength and Microstructural Properties of Fly Ash–Based Geopolymer Concrete,” *J. Mater. Civ. Eng.*, 2016.

[9] G. Sung *et al.*, “The mechanical properties of fly ash-based geopolymer concrete with alkaline activators,” *Constr. Build. Mater.*, vol. 47, no. 2013, pp. 409–418, 2015.

[10] N. K. Lee, J. G. Jang, and H. K. Lee, “Cement & Concrete Composites Shrinkage characteristics of alkali-activated fly ash/slag paste and mortar at early ages,” *Cem. Concr. Compos.*, vol. 53, pp. 239–248,

2014.

[11] P. Topark-Ngarm, P. Chindaprasirt, V. Sata, and P. C. and V. Sata, Pattanapong Topark-Ngarm, “Setting Time, Strength, and Bond of High-Calcium Fly Ash Geopolymer Concrete,” *J. Mater. Civ. Eng.*, vol. 27, no. 2011, pp. 1–7, 2015.

[12] D. Hardjito and S. E. Wallah, “On The Development of Fly Ash-based Geopolymer Concrete,” *ACI Mater. J.*, pp. 467–72, 2004.

[13] S. V. Patankar, Y. M. Ghugal, and S. S. Jamkar, “Effect of Concentration of Sodium Hydroxide and Degree of Heat Curing on Fly Ash-Based Geopolymer Mortar,” *Indian J. Mater. Sci.*, 2014.

[14] Manvendra Verma; Nirendra Dev, “Review on the effect of different parameters on behavior of Geopolymer Concrete,” *Int. J. Innov. Res. Sci. Eng. Technol.*, vol. 6, no. 6, pp. 11276–281, 2017.

[15] P. Nath and P. K. Sarker, “Effect of GGBFS on setting, workability and early strength properties of fly ash geopolymer concrete cured in ambient condition,” *Constr. Build. Mater.*, vol. 66, pp. 163–171, 2014.

[16] P. Rovnaník and S. O. Al, “Effect of curing temperature on the development of hard structure of metakaolin-based geopolymer,” *Constr. Build. Mater.*, vol. 24, no. 7, pp. 1176–1183, 2010.

[17] P. Nath and P. K. Sarker, “Flexural strength and elastic modulus of ambient-cured blended low-calcium fly ash geopolymer concrete,” *Constr. Build. Mater.*, vol. 130, pp. 22–31, 2017.

[18] S. Kumar, R. Kumar, and S. P. Mehrotra, “Influence of granulated blast furnace slag on the reaction, structure and properties of flyash-based geopolymer,” *J. Mater. Sci.*, pp. 607–615, 2010.

[19] A. Sathonsaowaphak, P. Chindaprasirt, and K. Pimraksa, “Workability and strength of lignite bottom ash geopolymer mortar,” *J. Hazard. Mater.*, vol. 168, pp. 44–50, 2009.

[20] Y. M. G. and S. V. P. S.S. Jamkar, “Effect of Fineness of Fly Ash on Flow and Compressive Strength of Geopolymer Concrete,” *Indian Concr. J.*, pp. 57–62, 2013.

[21] U. K. Salmabanu Luhar*, S. Luhar, and U. Khandelwal, “A Study on Water Absorption and Sorptivity of Geopolymer Concrete,” *SSRG Int. J. Civ. Eng.*, vol. 2, no. 8, pp. 1–10, 2015.

[22] P. S. Deb and P. K. Sarker, “Effects of Ultrafine Fly Ash on Setting, Strength, and Porosity of Geopolymers Cured at Room Temperature,” *Am. Soc. Civ. Eng.*, pp. 1–5, 2016.

[23] N. A. Lloyd and B. V Rangan, “Geopolymer Concrete with Fly Ash,” in *Second international conference on sustainable construction materials and technologies.*, 2017, no. January 2010.

[24] K. S. Finnie, D. S. Perera, O. Uchida, E. R. Vance, and K. S. Finnie, “Influence of curing schedule on the integrity of geopolymers,” *J. Mater. Sci.*, pp. 3099–3106, 2007.

[25] J. June *et al.*, “Engineering Properties of Alkali Activated Natural Pozzolan Concrete,” in *Second international conference on sustainable construction materials and technologies.*, 2010.

[26] J. G. Jang, N. K. Lee, and H. K. Lee, “Fresh and hardened properties of alkali-activated fly ash/slag pastes with superplasticizers,” *Constr. Build. Mater.*, vol. 50, pp. 169–176, 2014.

[27] K. U. Ambikakumari, M. Lahoti, and E. Yang, “Investigating the potential reactivity of fly ash for geopolymerization,” *Constr. Build. Mater.*, vol. 225, pp. 283–291, 2019.

[28] Y. D. T. C. Y. Dai, “Application of geopolymer paste for concrete repair,” *Struct. Concr.*, no. May 2018, pp. 1–11, 2017.

[29] Z. Pan, Æ. J. G. Sanjayan, J. G. Sanjayan, and A. B. V Rangan, “An investigation of the mechanisms for strength gain or loss of geopolymer mortar after exposure to elevated temperature,” *J. Mater. Sci.*, no. 44, pp. 1873–1880, 2009.

[30] D. D. Sakthidoss and T. Senniappan, “A Study on High Strength Geopolymer Concrete with Alumina-Silica Materials Using Manufacturing Sand,” *Silicon*, vol. 12, no. 3, pp. 735–746, 2020.

[31] B. V. Venkatarama Reddy and K. S. Jagadish, “Embodied energy of common and alternative building materials and technologies,” *Energy Build.*, vol. 35, no. 2, pp. 129–137, 2003.

[32] G. P. Hammond and C. I. Jones, “Embodied energy and carbon in construction materials,” *Proceedinds Inst. Civ. Eng.*, no. May, pp. 87–98, 2008.

[33] K. Kupwade-Patil, C. De Wolf, S. Chin, and J. Ochsendorf, “Impact of Embodied Energy on Materials / Buildings with Partial Replacement of Ordinary Portland Cement (OPC) by Natural Pozzolanic Volcanic Ash Impact of Embodied Energy on materials/buildings with partial replacement of ordinary Portland Cement (OP,” *J. Clean. Prod.*, no. January 2018, pp. 1–9, 2017.

[34] Bureau of Indian Standards, “43 GRADE ORDINARY PORTLAND CEMENT - SPECIFICATION,” *IS 81121989*, no. May, 1990.

[35] Bureau of Indian Standard, “Determination of Initial and Final Setting Time,” *IS 4031 (Part 5)*, vol. 4031, no. 1, pp. 3–6, 2002.

[36] Bureau of Indian Standard, “METHODS OF PHYSICAL TESTS FOR HYDRAULIC CEMENT PART II Determination of Density,” *IS 4031(Part 11)*, vol. 4031, pp. 1–2, 1995.

[37] Bureau of Indian Standard, “Fineness by dry sieving,” *IS 4031 (Part I)*, vol. 4031, 1996.

[38] Bureau of Indian Standard, “Determination of Soundness,” *IS 4031 (Part 3)*, vol. 4031, no. 1, pp. 2–7, 2002.

[39] Bureau of Indian Standard, “Determination of Consistency of Standard Cement Paste,” *IS 4031 (Part 4)*, vol. 4031, no. August 1988, 1997.

[40] Bureau of Indian Standard, “Determination of False Set,” *IS 4031 (Part 14)*, vol. 4931, 1999.

[41] ASTM International, “Standard Specification for Coal Fly Ash and Raw or Calcined Natural Pozzolan for Use,” *C618 − 19*, pp. 1–5, 2019.

[42] Bureau of Indian Standard, “Mechanical Properties,” *IS 2386(Part IV)*, vol. 2386, no. March 1964, 1997.

[43] Bureau of Indian Standard, “Estimation of Deleterious Materials and Organic Impurities,” *IS 2386 (Part II)*, vol. 2386, no. October 1963, 1998.

[44] Bureau of Indian Standard, “Coarse and Fine Aggregate from Natural Sources for Concrete,” *IS 383-1970*, no. 1997, pp. 1–20, 1997.

[45] Bureau of Indian Standard, “Particle Size and Shape,” *Is 2386(Part I)*, vol. 2386, 1997.

[46] Bureau of Indian Standard, “Specific Gravity, Density, Voids, Absorption and Bulking,” *IS 2386 (Part III)*, vol. 2386, no. October 1963, 1997.

[47] Bureau of Indian Standard, “MEASURING MORTAR MAKING PROPERTIES OF FINE AGGREGATE,” *IS 2386 (Part VI)*, vol. 2386, no. October 1963, 1997.

[48] Bureau of Indian Standard, “Soundness,” *IS 2386*, 1997.

[49] ASTM International, “Standard Test Method for Materials Finer than 75-µm (No . 200) Sieve in Mineral Aggregates by Washing,” *C117 − 17 Stand.*, no. 200, pp. 7–10, 2019.

[50] ASTM International, “Standard Test Method for Surface Moisture in Fine Aggregate,” *C70 − 13*, pp. 1–3, 2019.

[51] ASTM International, “Standard Test Method for Bulk Density (‘ Unit Weight ’) and Voids in Aggregate,” *C29/C29M − 17a*, pp. 1–5, 2019.

[52] ASTM International, “Standard Test Method for Sieve Analysis of Fine and Coarse Aggregates,” *C136/C136M − 14*, pp. 1–5, 2019.

[53] ASTM International, “Standard Test Method for Relative Density (Specific Gravity) and Absorption of Fine,” *C127 − 15*, pp. 1–6, 2019.

[54] Bureau of Indian Standards, “CONCRETE ADMIXTURES-Specification,” *IS 91031999*, vol. April, 1999.

[55] M. Verma and M. Nigam, “Mechanical Behaviour of Self Compacting and Self Curing Concrete,” *Int. J. Innov. Res. Sci. Eng. Technol.*, vol. 6, no. 7, pp. 14361–366, 2007.

[56] Bureau of Indian Standard, “METHODS OF TEST FOR STRENGTH OF CONCRETE,” *IS 516-1959*, 2004.

[57] Bureau of Indian Standard, “SPECIFICATION FOR MOULDS FOR USE IN TESTS OF CEMENT AND CONCRETE,” *IS 10086 - 1982*, no. 1952, 2008.

[58] Bureau of Indian Standard, “SPLITTING TENSILE STRENGTH OF CONCRETE - METHOD OF TEST,” *IS 5816 1999*, 1999.

[59] Bureau of Indian Standard, “SPECIFICATION FOR APPARATUS FOR FLEXURAL TESTING OF CONCRETE,” *IS9399 - 1979*, no. 2004, 1979.

[60] Bureau of Indian Standards, “Method of non-destructive testing of concrete-methods of test Part 2: Rebound hammer,” *Is 13311-2*, no. 2004, 1992.

[61] Bureau of Indian Standard, “Non-destructive testing of concrete methods of test Part 1: Ultrasonic pulse velocity,” *IS 13311 (Part1) 1992*, no. 2004, 1992.

[62] M. Albitar, P. Visintin, M. S. M. Ali, M. Drechsler, M. S. Mohamed Ali, and M. Drechsler, “Assessing Behaviour of Fresh and Hardened Geopolymer Concrete Mixed with Class-F Fly Ash,” *KSCE J. Civ. Eng.*, vol. 19, pp. 1445–1455, 2015.

[63] Manvendra Verma; Nirendra Dev, “Effect of SNF-Based Superplasticizer on Physical, Mechanical and Thermal Properties of the Geopolymer Concrete,” *Silicon*, pp. 1–11, 2021.

[64] S. Demie, M. F. Nuruddin, N. Shafiq, M. Fadhil, and N. Shafiq, “Effects of microstructure characteristics of interfacial transition zone on the compressive strength of self-compacting geopolymer concrete,” *Constr. Build. Mater.*, vol. 41, no. 2013, pp. 91–98, 2020.

[65] D. L. Y. Kong and J. G. Sanjayan, “Cement and Concrete Research Effect of elevated temperatures on geopolymer paste, mortar and concrete,” *Cem. Concr. Res.*, vol. 40, no. 2, pp. 334–339, 2010.

[66] M. Verma and N. Dev, “Sodium hydroxide effect on the mechanical properties of flyash-slag based geopolymer concrete,” *Struct. Concr.*, pp. 1–12, 2020.

[67] H. G. Russell *et al.*, “State-of-the-Art Report on High-Strength Concrete Reported by ACI Committee 363,” vol. 92, no. Reapproved, 1997.

[68] “ceb-fip-model-code-1990-design-code.pdf.” 1990.

[69] A. C. I. Committee, *Building Code Requirements for Structural Concrete (ACI 318-14)*. 2014.

[70] C. Concrete, *Reinforced Concrete Design in accordance with AS 3600—2009*. 2009.

[71] Bureau of Indian Standard, “PLAIN AND REINFORCED CONCRETE - CODE OF PRACTICE,” *IS 4562000*, no. July, 2000.

[72] J. K. R. VARSHA BN, SARANYA S, “EMBODIED ENERGY OF AGGREGATES AND MASONRY UNITS PRODUCED AROUND BENGALURU, INDIA,” *Int. J. Adv. Sci. Eng. Technol.*, vol. 6, no. 1, pp. 42–45, 2018.

[73] L. G. Breitenbach, U. Ppgem, and F. Kirch, “A case study about embodied energy in concrete and structural masonry buildings,” *J. Constr.*, vol. 13, no. 2, pp. 9–14, 2014.

[74] S. R. Anvekar, L. R. Manjunatha, S. R. Anvekar, S. Sagari, and K. Archana, “An Economic and Embodied Energy Comparison of Geopolymer, Blended Cement and Traditional Concretes,” *J. Civ. Eng. Technol. Res.*, vol. 1, no. November, pp. 33–40, 2014.

Tables

Table 1 Cement Properties

Test	Result	As per IS 4031-1998
Consistency	30%	30-35
Initial setting time	40 min	Not less than 30min.
Final setting time	1 hr 20 min	Not more than 600min
Specific gravity	3.15	3.10-3.15
Fineness	2.9%	Not exceed 10%
soundness	2mm	Not exceed 10mm

Table 2 Composition of Flyash and GGBFS

Characteristics	SiO_2	Al_2O_3	CaO	Fe_2O_3	MgO	SO_3	LOI
Flyash (%)	45.8	21.4	13.7	12.6	1.3	1.9	.1
GGBFS (%)	34.52	20.66	32.43	.57	10.09	.77	.3

Table 3 Properties of Fine Aggregate/Stone Dust (M-Sand).

S.No.	Test	Results	As Per IS
1.	Zone	Zone II	IS: 2386 (Part I)-1963
2.	Grade	Well Graded	IS: 2386 (Part I)-1963
3.	Fineness Modulus	2.756 (Medium sand)	2.6-2.9 [IS: 2386 (Part I)-1963]
4.	Specific Gravity	2.62	2.6-2.8 [IS: 2386 (Part III)-1963]
5.	Water absorption	1.21 %	Less than 3% [IS: 2386 (Part III)-1963]
6.	Silt Content	6 %	Less than 8% [IS: 2386 (Part I)-1963]
7.	Bulk density	1610 kg/m^3	IS: 2386 (Part III)-1963

Table 4 Properties of coarse Aggregate.

S. No.	Test	Results	As per IS
1.	Fineness Modulus	7.29	6 - 9 [IS: 2386 (Part I)-1963]
2.	Specific Gravity	2.79	2.6-2.8 [IS: 2386 (Part III)-1963]
3.	Water absorption	0.2%	Less than 2% [IS: 2386 (Part III)-1963]
4.	Crushing Value	23%	Less Than 30% [IS: 2386 (Part-IV)-1963]
5.	Impact Value	22%	Less Than 30% [IS: 2386 (Part-IV)-1963]
6.	Flakiness Index	24%	Less than 30% [IS: 2386 (Part I)-1963]
7.	Elongation Index	30%	Less than 45% [IS: 2386 (Part I)-1963]
8.	Abrasion value	8%	Less Than 16% [IS: 2386 (Part-IV)-1963]

Table 5 Properties of Superplasticiser.

S. No.	**Test**	**Results**
1.	Appearance	Brown liquid
2.	Specific gravity	1.18 @ 25°C
3.	Chloride content	Nil to BS 5075 / BS: EN934
4.	Air entrainment	Less than 2% additional air entrained at usual dosages.

Table 6 Mix Proportion of GPC and OPC concrete

Constituents	OPC Concrete Mix Content (kg/m^3)	Geopolymer Concrete Mix Content (kg/m^3)
OPC	370	00
Flyash	00	303.75
GGBFS	00	101.25
NaOH	00	40.5
Na_2SiO_3	00	101.25
Fine Aggregate	683	683
Coarse Aggregate	1289	1269
Water	148	40.5
Superplasticiser	3.7	4.05
Total	2493.7	2543.7

Table 7 Embodied energy calculation of GPC and OPC

Constituents	Embodied Energy (MJ/kg)	OPC Concrete		Geopolymer Concrete	
		Mix Content (kg/m^3)	Embodied Energy Content (MJ/kg)	Mix Content (kg/m^3)	Embodied Energy Content (MJ/kg)
OPC	4.6	370	1702	-	-
Flyash	0.0	-	-	303.75	00
GGBFS	0.2	-	-	101.25	31.38
NaOH	20.5	-	-	40.5	830.25
Na_2SiO_3	5.37	-	-	101.25	543.71
Fine Aggregate	0.02	683	13.66	683	13.66
Coarse Aggregate	0.22	1289	283.58	1269	279.18
Water	0.0	148	00	40.5	00
Superplasticiser	12.6	3.7	46.62	4.05	51.03
	Total	2493.7	2045.86 MJ/m^3	2543.7	1749.21 MJ/m^3

Table 8 Cost analysis of the GPC and OPC concrete

Constituents	Cost rate (Rs./kg)	OPC Concrete		Geopolymer Concrete	
		Mix Content (kg/m^3)	Cost of the Constituent ($Rs./m^3$)	Mix Content (kg/m^3)	Cost of the Constituent ($Rs./m^3$)
OPC	7.6	370	2812	-	-
Flyash	0.7	-	-	303.75	212.62
GGBFS	2.5	-	-	101.25	253.13
NaOH	10.05	-	-	40.5	407.03
Na_2SiO_3	10	-	-	101.25	1012.5
Fine Aggregate	0.25	683	170.75	683	170.75
Coarse Aggregate	0.525	1289	676.72	1269	666.23
Water	0.0	148	00	40.5	00
Superplasticiser	26.67	3.7	98.68	4.05	108.01
	Total	2493.7	Rs. 3758.15/m^3	2543.7	Rs. 2230.27/m^3

Figures

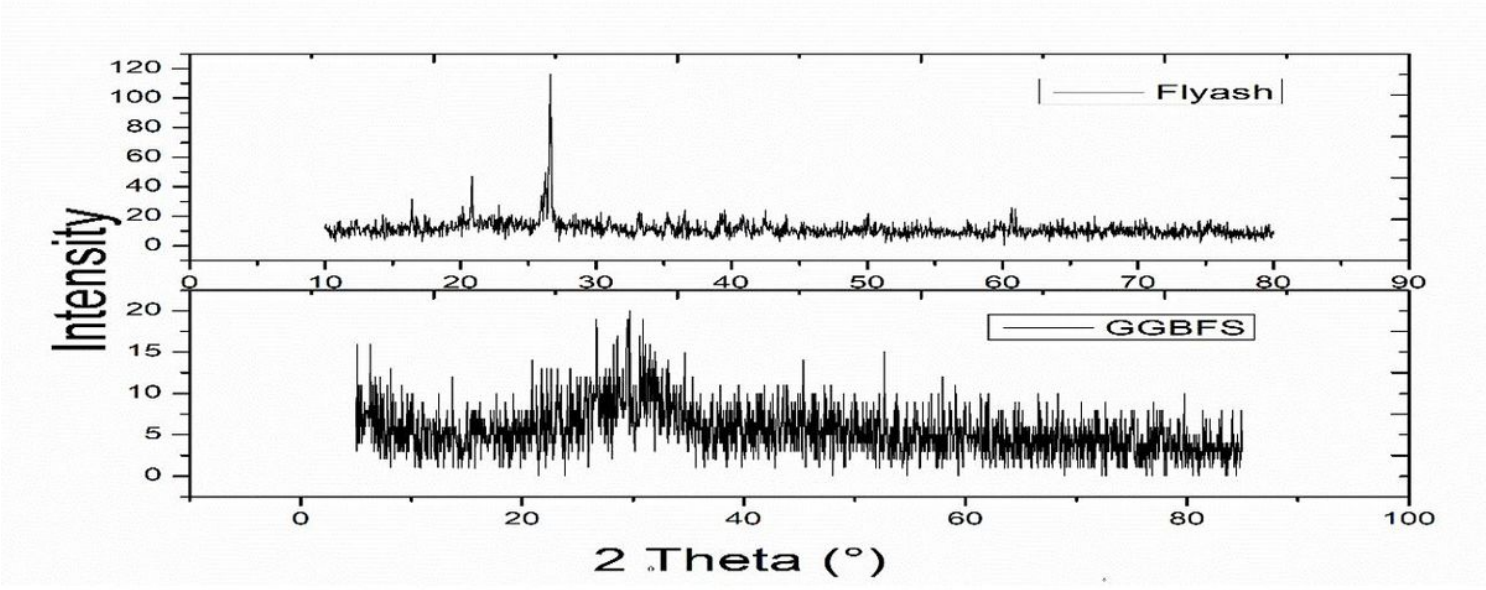

Figure 1

XRD pattern of flyash and GGBFS

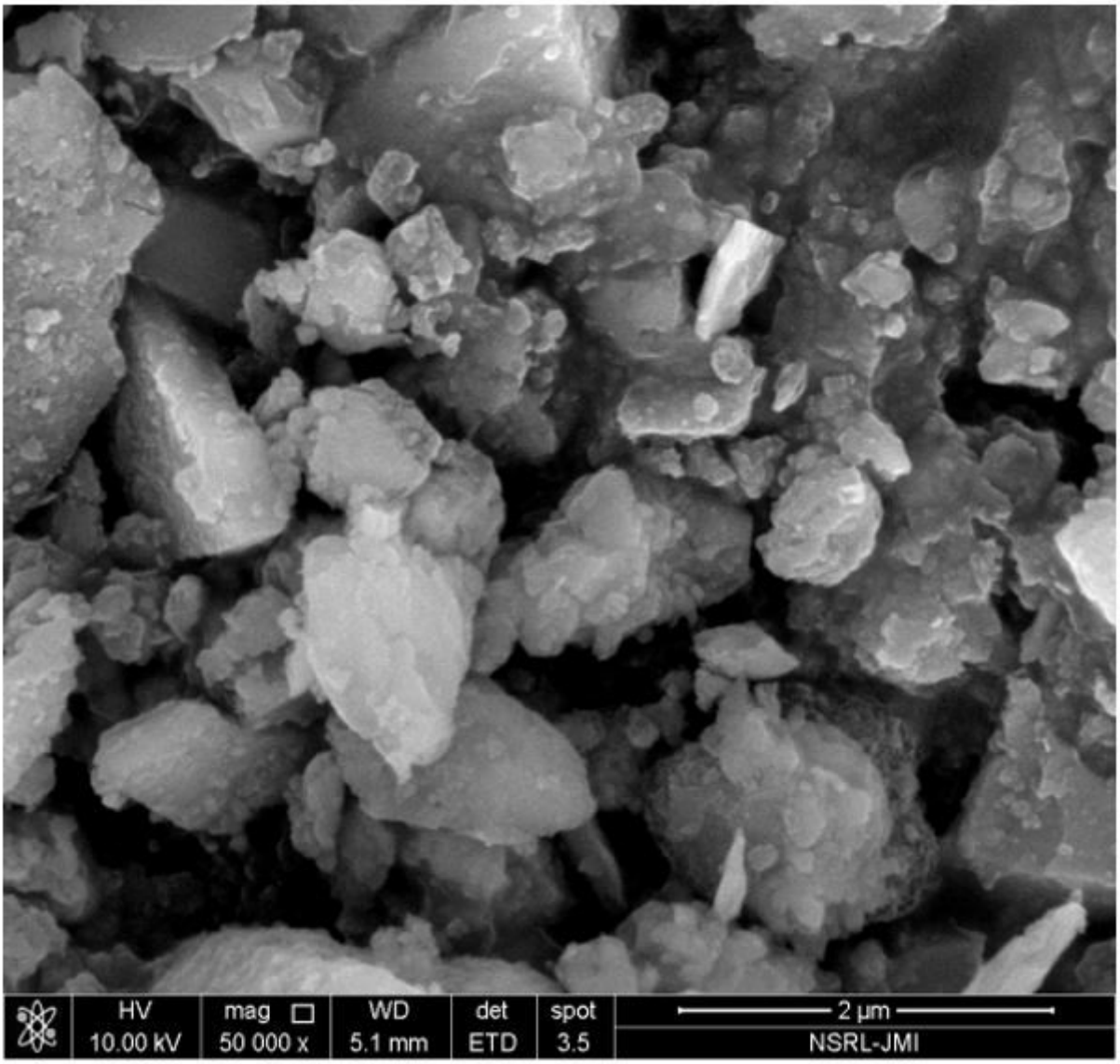

Figure 2

SEM image of GGBFS

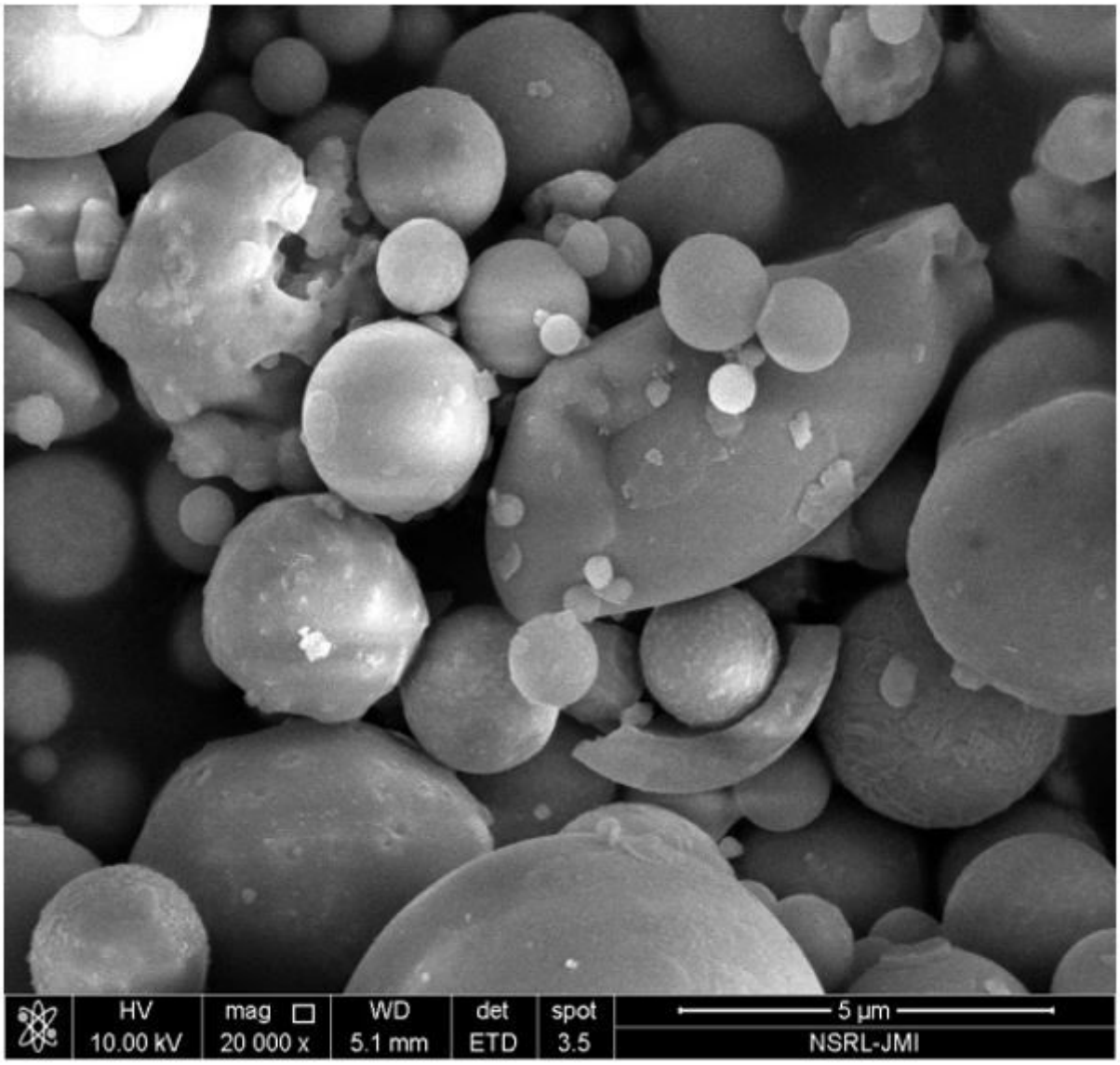

Figure 3

SEM image of flyash

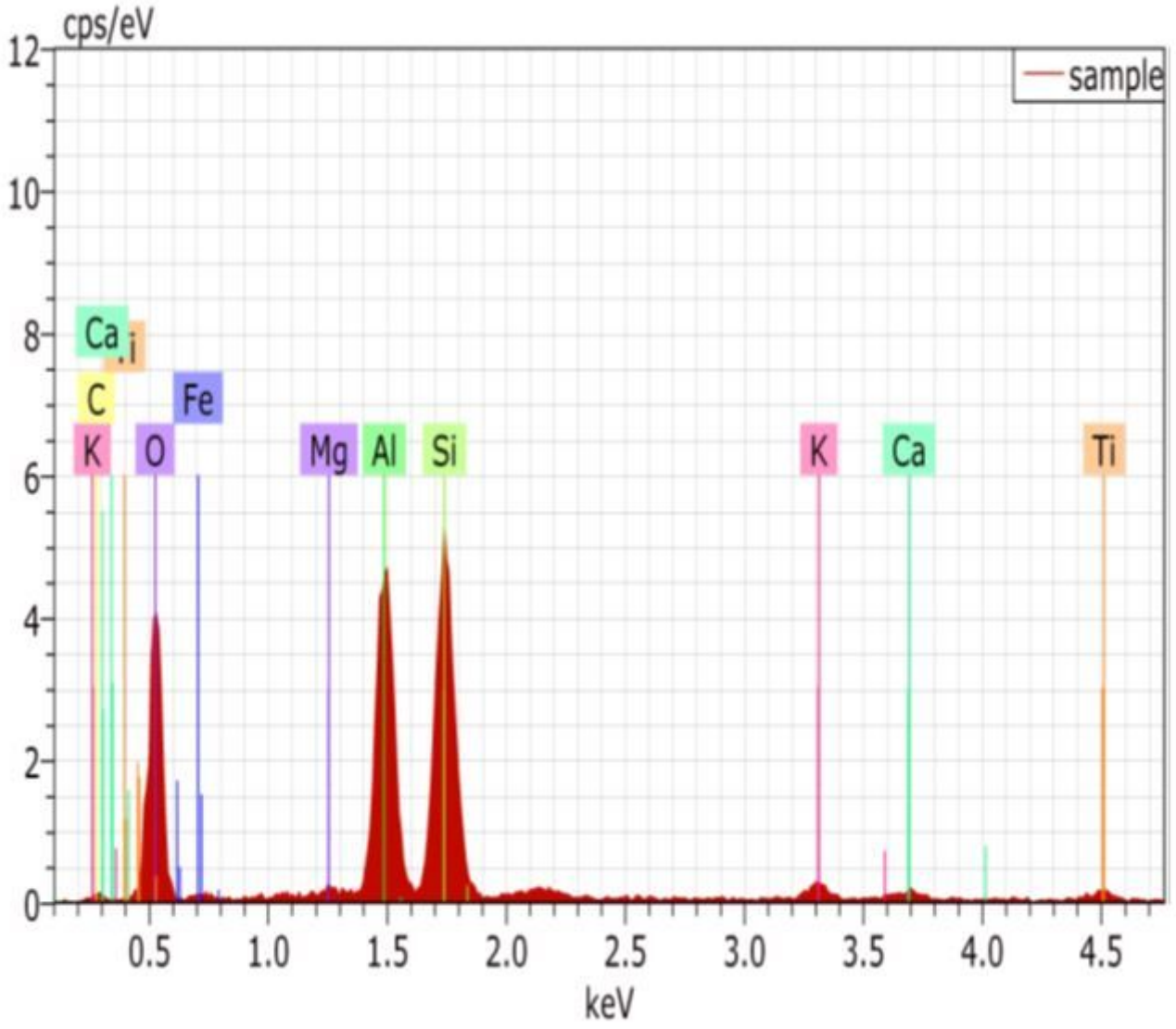

Figure 4

EDS graph of flyash

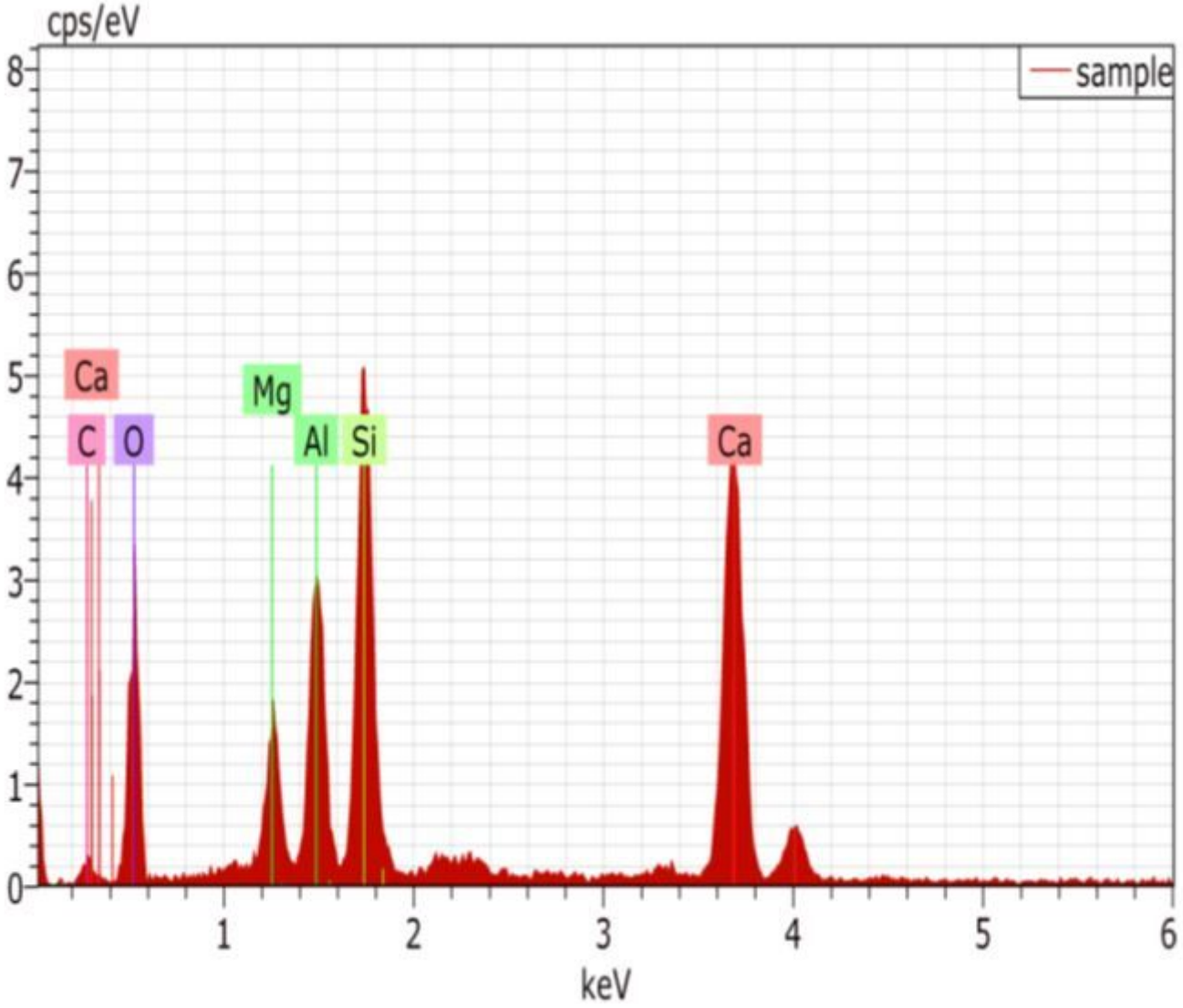

Figure 5

EDS graph of GGBFS

Figure 6

Picture of sodium hydroxide flakes

Figure 7

Picture of sodium silicate solutions

Figure 8

Stone-dusts or fine aggregate

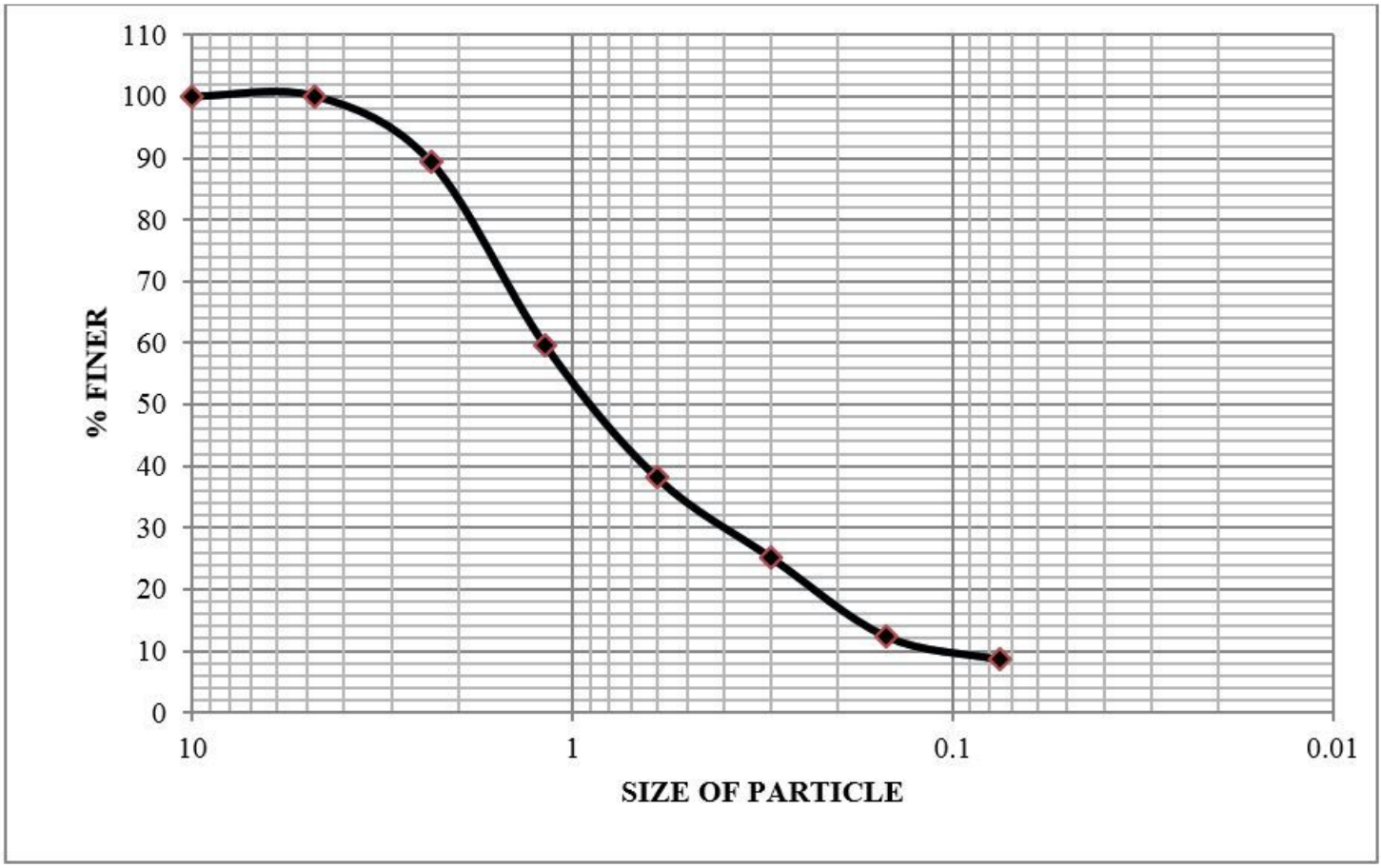

Figure 9

Grain size distribution curve

Figure 10

Coarse aggregates raw sample picture.

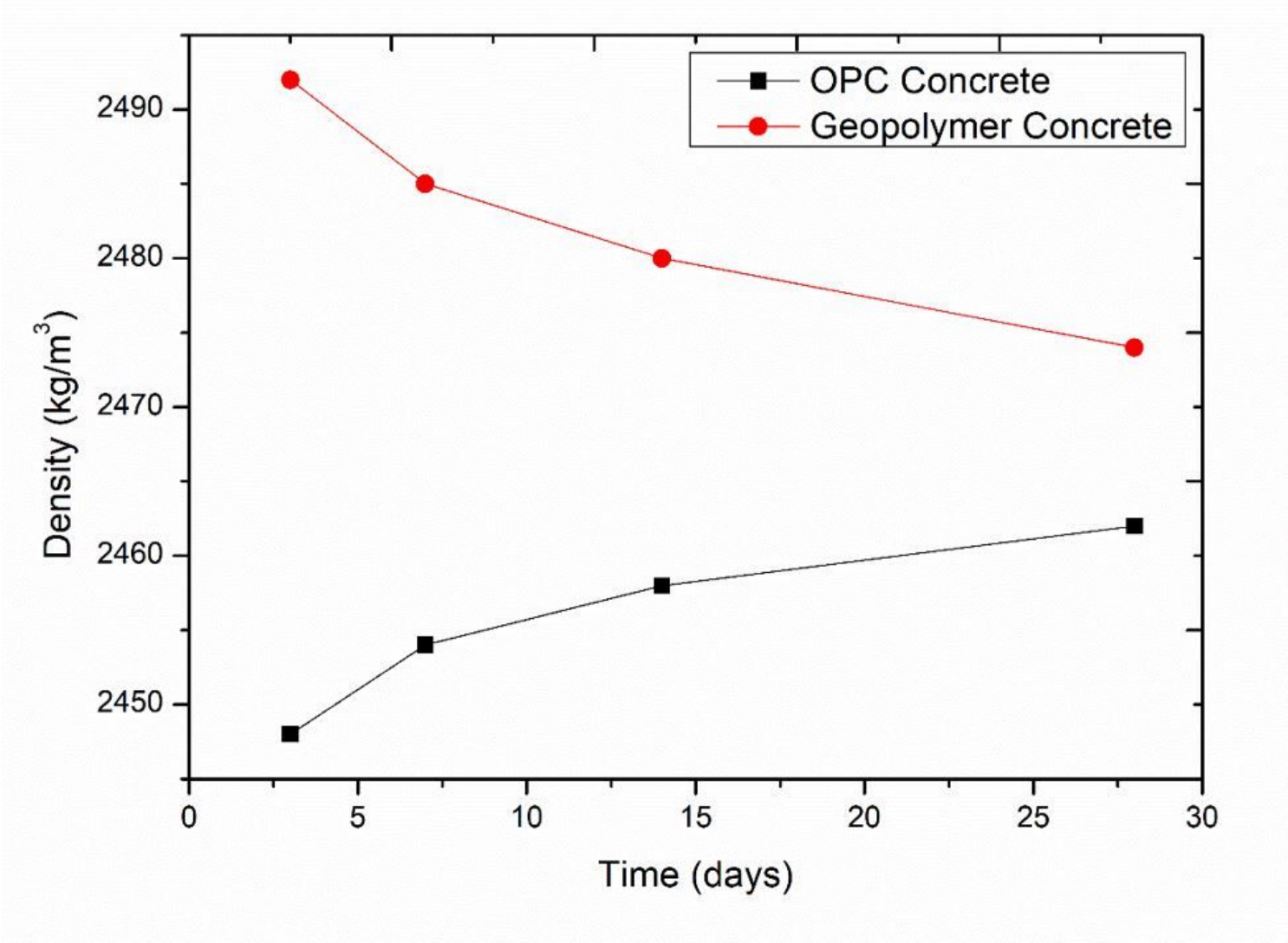

Figure 11

Density variations with time

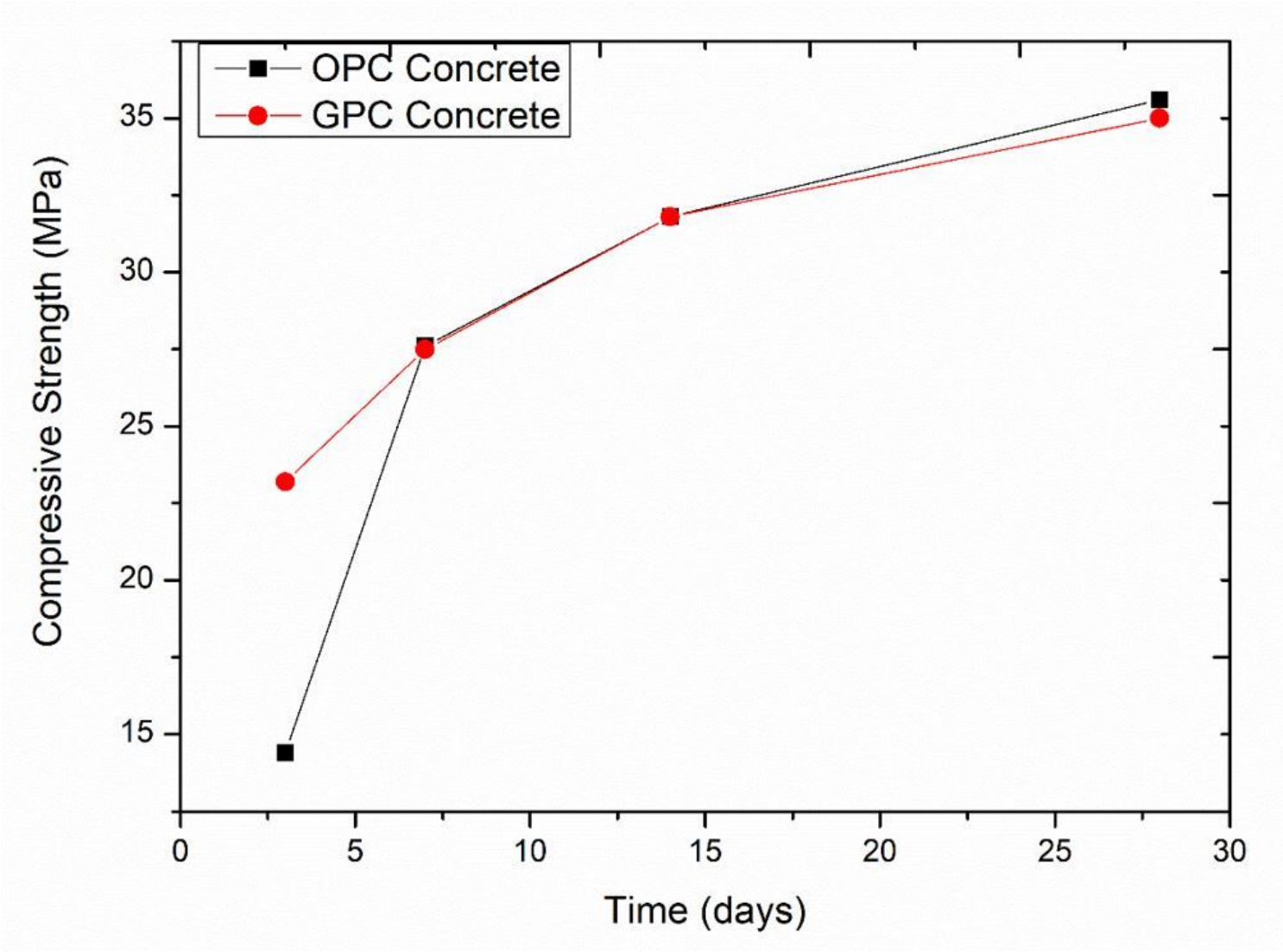

Figure 12

Compressive strength of GPC and OPC concrete

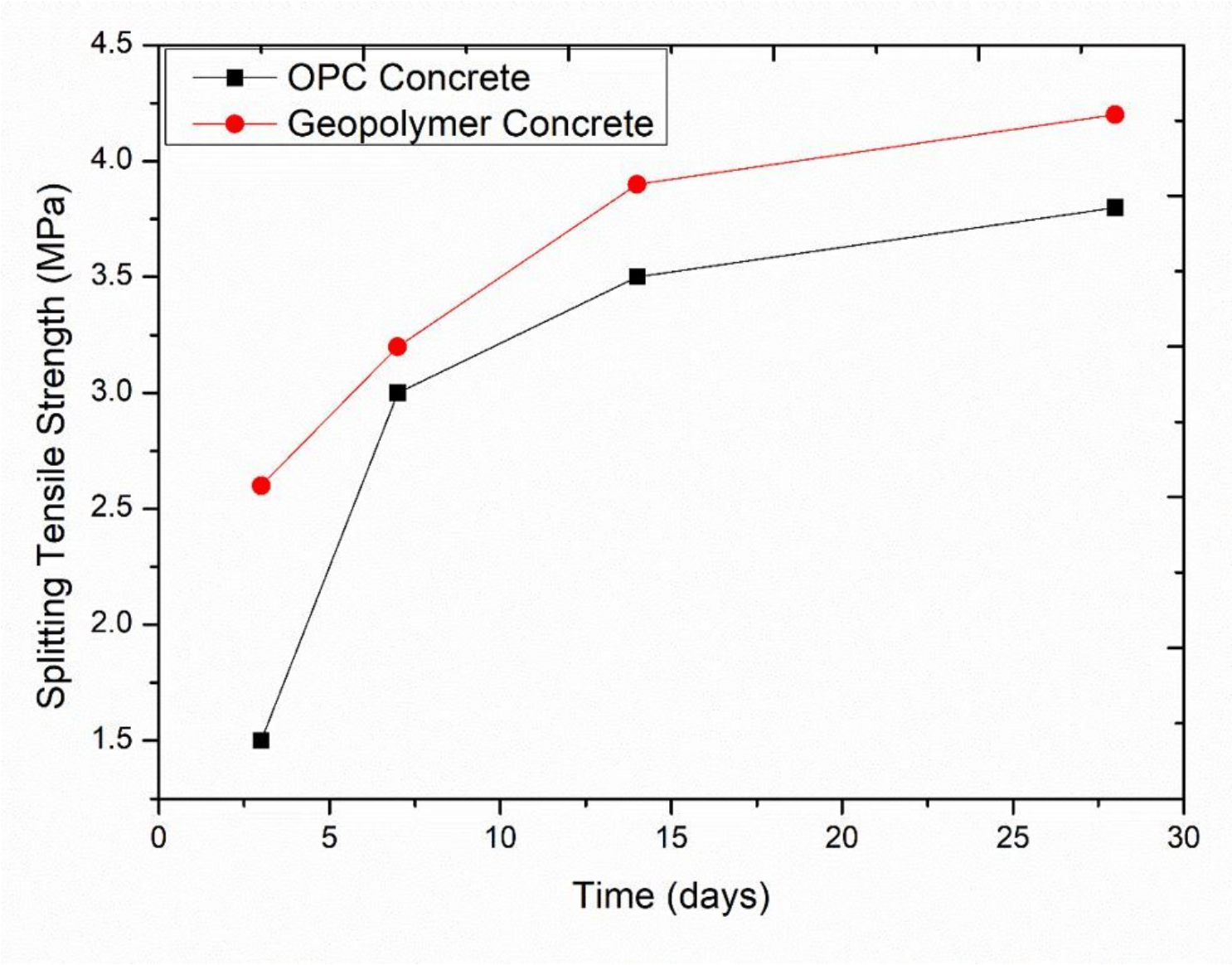

Figure 13

Splitting tensile of the GPC and OPC concrete

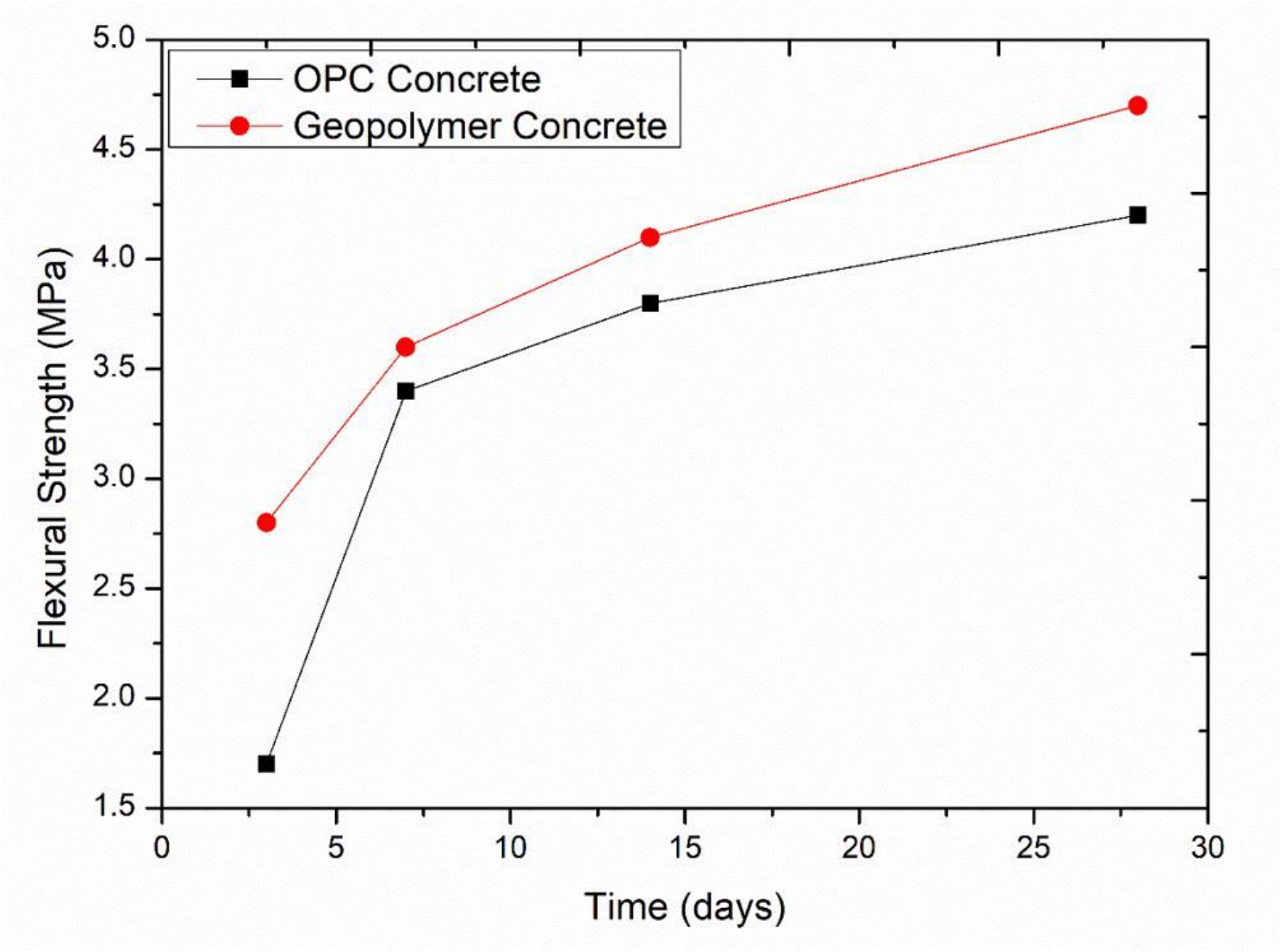

Figure 14

Flexural strength of GPC and OPC concrete

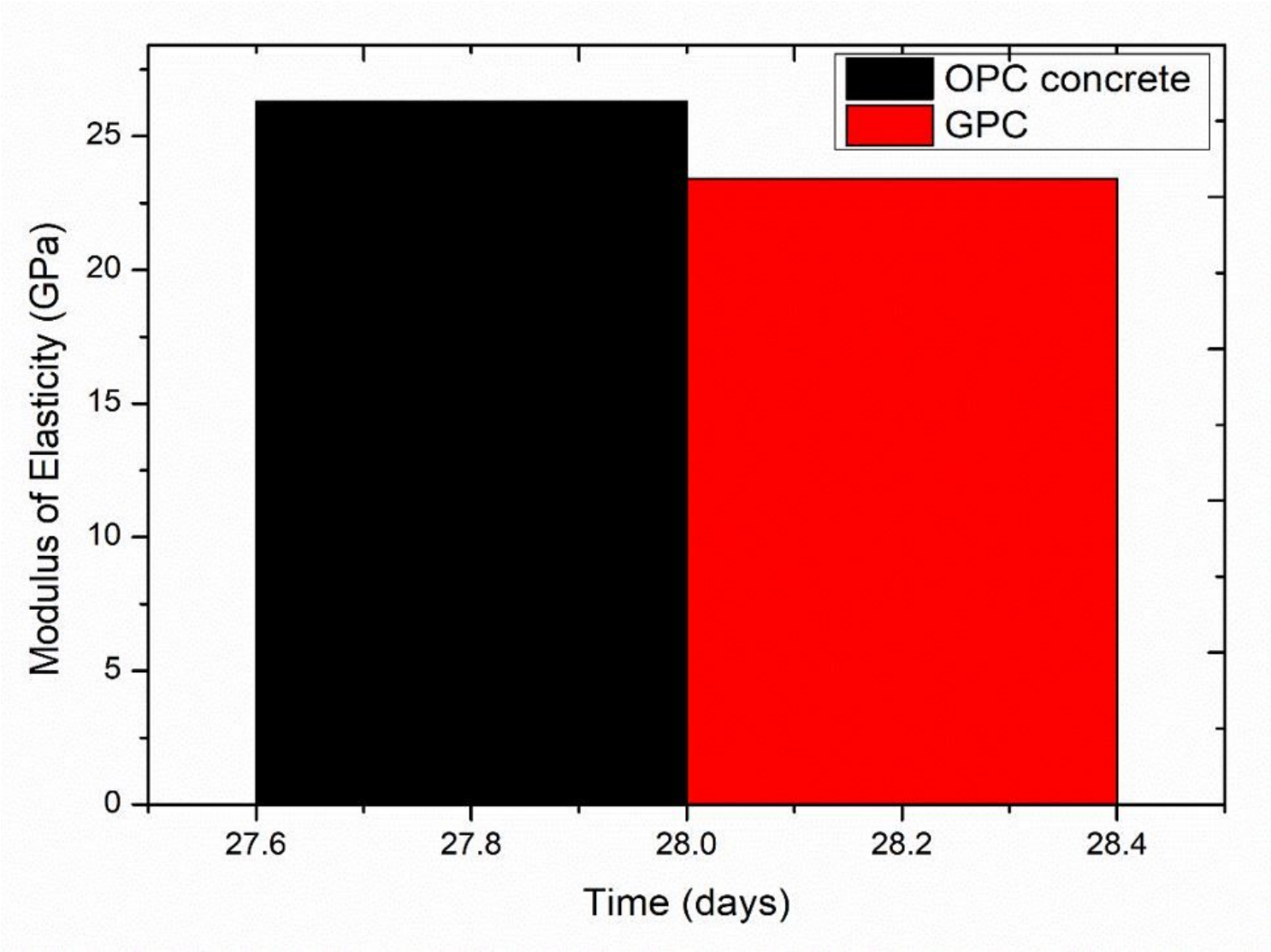

Figure 15

Graph Modulus of Elasticity of OPC concrete and GPC

Figure 16

Poisson’s ratio test setup

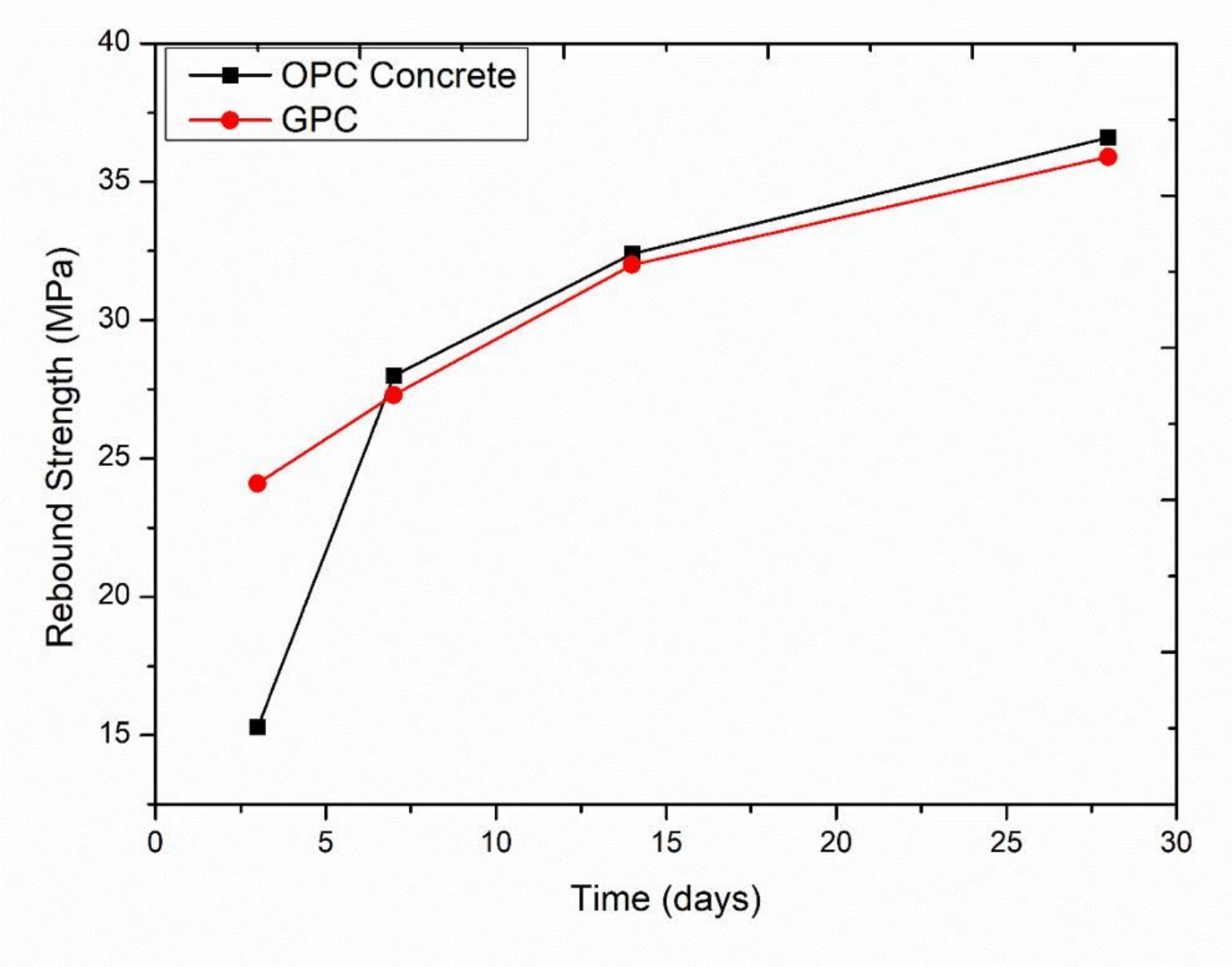

Figure 17

Graph of OPC concrete and GPC Rebound Strength

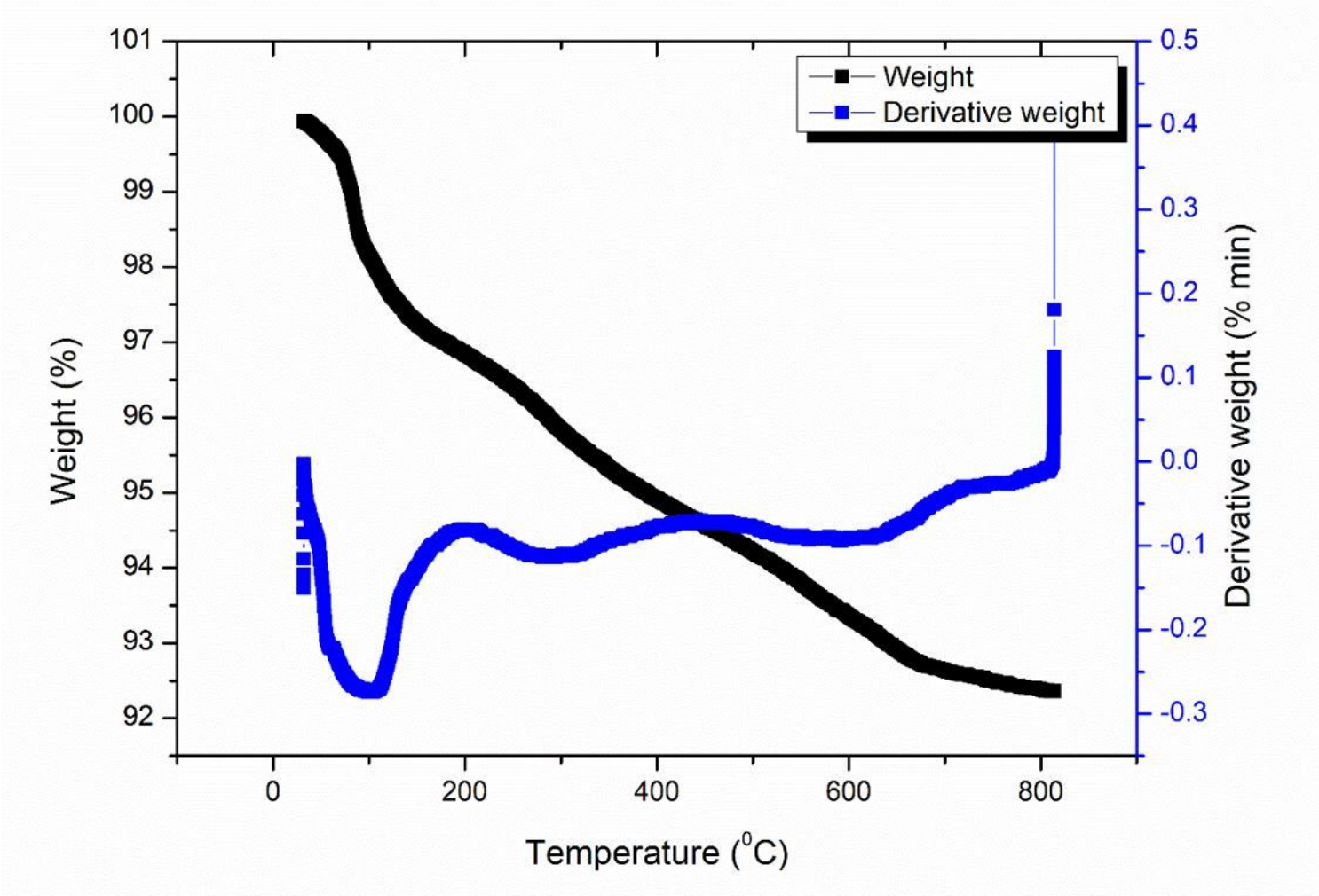

Figure 19

Graph of TGA-DTG test of GPC mix

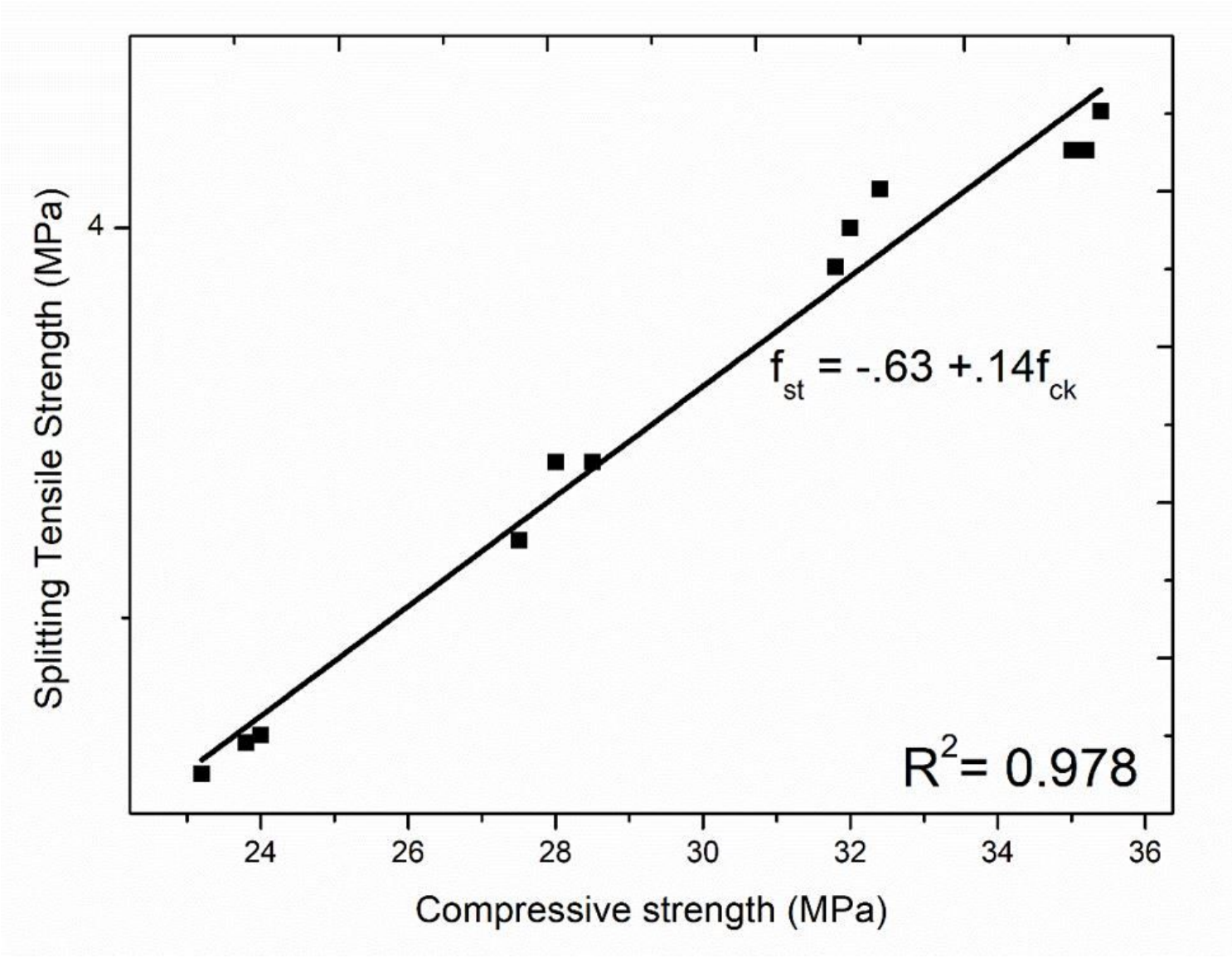

Figure 20

Graph of Correlation between compressive strength and splitting tensile

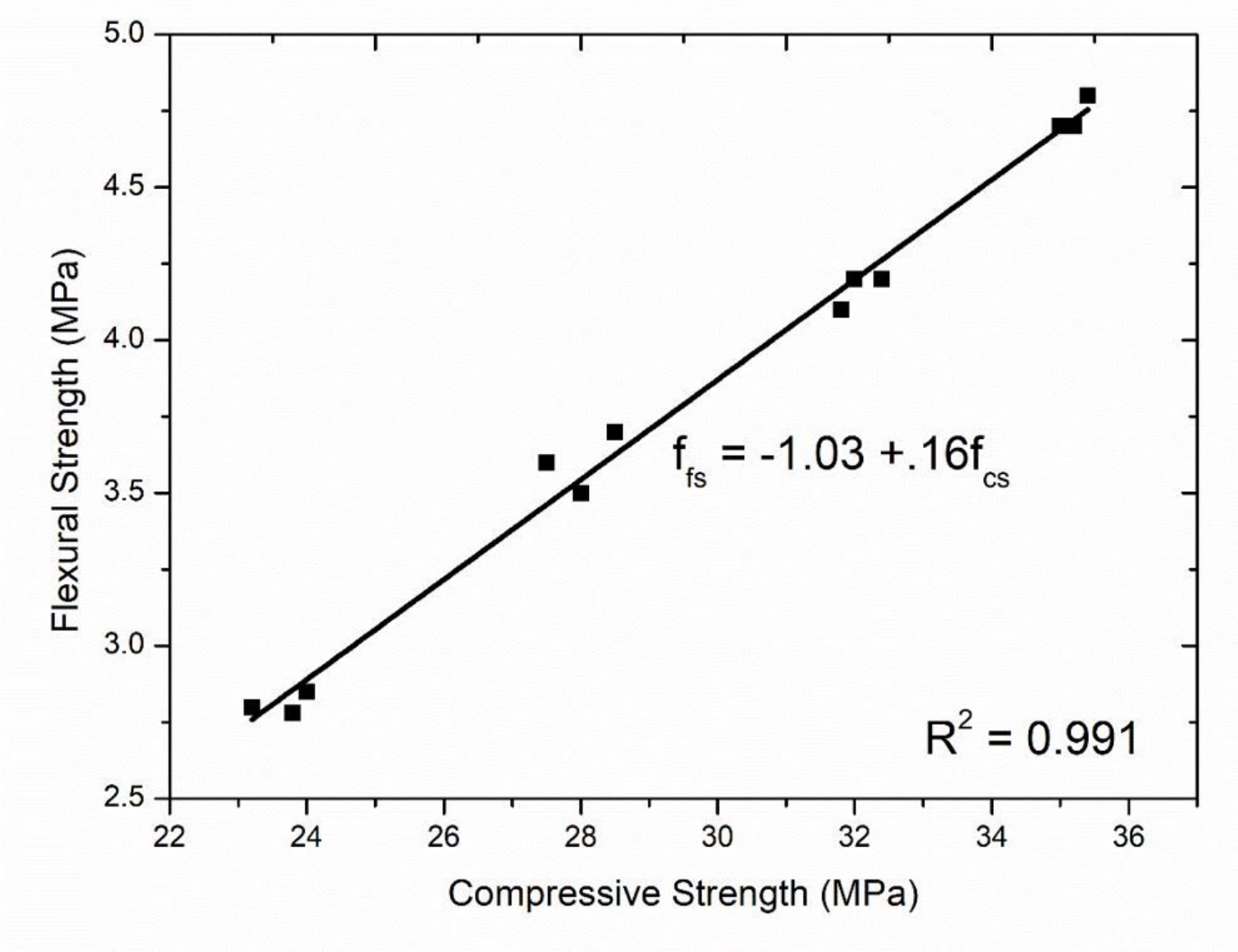

Figure 21

Graph of Correlation between compressive strength and flexural strength